

# THE EFFECT OF MATERIAL STIFFNESS ON DENTAL IMPLANT STABILITY – A FINITE ELEMENT ANALYSIS

Muhammad Ikman Ishak<sup>a\*</sup>, Ruslizam Daud<sup>a</sup>, Siti Noor Fazliah Mohd Noor<sup>b</sup>

<sup>a</sup>Faculty of Mechanical Engineering & Technology, Universiti Malaysia Perlis (UniMAP), Kampus Alam UniMAP, Pauh Putra, 02600 Arau, Perlis, Malaysia

<sup>b</sup>Advanced Medical and Dental Institute, Universiti Sains Malaysia, Bertam, Jln. Tun Hamdan Sheikh Tahir, 13200 Kepala Batas, Pulau Pinang, Malaysia

## Article history

Received

10 December 2021

Received in revised form

23 February 2022

Accepted

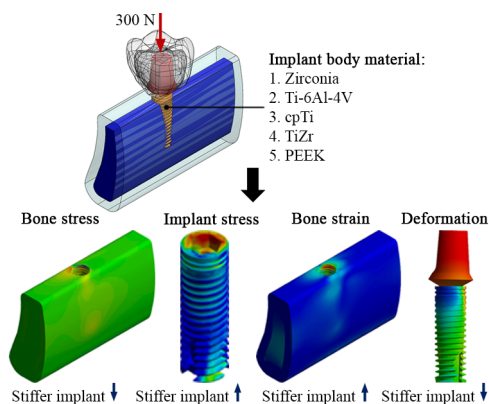
01 March 2022

Published online

28 February 2023

\*Corresponding author  
ikman@unimap.edu.my

## Graphical abstract



## Abstract

The perseverance of dental implant system in restoration of occlusion is highly dependent on biomechanical overloading factors such as implant macro geometries, parafunctional oral habits, and material. Different implant materials could affect the load transfer at the bone-implant interface differently which is related to stress shielding phenomenon. To date, the role of various implant materials on the surrounding tissues as well as implant stability is still debatable and unclear especially when the implant failure is of concern. Through this study, implant body with different materials or stiffnesses that are zirconia, Ti-6Al-4V, cpTi, TiZr, and PEEK were investigated via 3-D FEA. The bone tissues were modelled based on CT image datasets and subsequently be processed in SolidWorks software. All geometries were converted into finite element models and analysed in ANSYS software. The bone and implant models were assigned with anisotropic and isotropic properties, respectively. A dynamic occlusal loading of 300 N and pretension of 20 N were applied on the implant body and screw, respectively. The results showed that the less stiff implant increased the bone stress and decreased the implant body stress values compared to the stiffer implant. Moreover, the implant with lower stiffness exhibited lower bone strain and higher implant deformation than the implant with higher stiffness. Of all implant materials analysed, PEEK is observed to be the most satisfactory. However, further modifications on PEEK would be necessary to improve inherent bioactivity and osseointegration.

**Keywords:** Deformation, dental implant, finite element analysis, material stiffness, stress

© 2023 Penerbit UTM Press. All rights reserved

## 1.0 INTRODUCTION

An implant system designated for use in replacing missing teeth is defined as a dental implant commonly used in prosthodontics which is inserted into the soft and hard oral tissues to provide retention or support for a fixed or removable prosthesis. A standard osseointegrated dental implant comprises three main individual components which are implant body, abutment, and abutment screw. The dental implant is used to attach the artificial tooth (prosthesis or crown) to the jawbones so that the biting and chewing forces can be distributed. It is one of the best treatment options for patients to restore the missing teeth in terms of function, comfort, and aesthetic. The success of dental implant has well been evidenced over years through many clinical follow-up studies [1, 2]. However, the post-placement complications that leading to implant failures such

as the fracture and loosening of abutment and implant body still occur. The fracture of implant body is more infrequent than the loosening and fracture of abutment and screw. Although the implant body fracture is scarce which accounts for 0.2 – 1.5% [3], their impact is highly frustrating not only for patients, but also for dental surgeons [4]. The loss of implant normally demands maintenance and further corrective measures including a new period of rehabilitation.

There are two main factors contributing to the implant complications which are technical overloading and biological-related incidences. The technical overloading is found to leave a more significant effect on the implant stability compared to the biological-related event. This may be associated with several inadequate implant biomechanical aspects that weakening the bone-implant connection, supported with the absence of the periodontal ligaments to sustain the

physiological loading. Uncommon response of the implant towards loading could result in marginal bone loss and subsequent collapse of the prosthesis or implant parts. Besides, soft tissue deformation, aesthetic compromise, and patient dissatisfaction are other implications [5]. Concerning these issues, it is a necessity to ensure that the bone-implant interaction due to biomechanical overloading factors exhibits responses within the permissible physiological tolerance. The material, length, diameter [3] and cervical wall thickness of the implant body [6], abutment height, and parafunctional oral habits [7] are the most common biomechanical overloading factors identified to cause implant instability. Hence, material used to fabricate the implant is of interest as it is related towards load transfer and implant stability.

The material utilised in dental implant fabrication must achieve mechanical, physical, and biological needs because the implant is in direct attachment with living tissues and considerably be loaded with occlusal force. The material of implant supposedly acquires properties that close to the bone to prevent low bone stress adaptation because of stress shielding effect. Ceramics and titanium are the typical materials chosen in the fabrication of dental implant [8]. For commercially pure titanium (cpTi), grade IV exhibits the highest strength compared to others and being the reason of why it has extensively been used in the market [9]. Moreover, titanium alloy (Ti-6Al-4V) which categorised under grade V, has an improved yield strength and fatigue resistance, also making it as one of the prominent materials. Ceramics such as zirconia, on the other hand, promote a more aesthetic option than titanium in fulfilling the demands and expectations of the patient [9]. Current implant manufacturing also considers zirconia alloy with titanium or also known as titanium zirconium (TiZr) which having better tensile strength, hardness, corrosion resistance, and biocompatibility compared to pure materials [10]. Besides, polymers and polymeric reinforced composites (polyetheretherketone (PEEK)) are new emerging materials with the lowest elastic modulus (3 – 4 GPa) relative to other implant materials [9, 11]. The PEEK is highly biocompatible, resistant to hydrolysis, and exhibits good thermal, mechanical, and chemical abrasions resistance [12]. However, the influence of different materials on the implant stability remains a subject of debate and unclear. Further to that, lack of information is available regarding the suitable selection of implant material, and subsequently the emphasise on implant design prior to implant fabrication.

Computational analysis currently is popular and well accepted technique for examining the biomechanical characteristics including stress and strain alterations. It is easier and more flexible than experimental tests. Finite element analysis (FEA) is widely used computational method in dental implantology that allows investigators to predict the responses which are challenging to be determined in *in vitro* and *in vivo* works especially at the bone-implant interface [13-15]. FEA plays an important role in explaining mathematical modelling problems in many fields of science and industry such as through structural, fluid [16, 17], thermal, fatigue, and fracture mechanics analyses [18-22].

Thus, this study was aimed in evaluating the mechanical responses of a dental implant in terms of stress, strain, and deformation among five different types of implant materials which are zirconia, Ti-6Al-4V, cpTi, TiZr, and PEEK using three-dimensional (3-D) FEA. It is hoped that this study will provide

an improved understanding on load transfer at the bone-implant interface and subsequently addressed the issue of implant instability which leads to failure. Besides, improving materials with low elastic modulus may be a key factor in reducing implant failure and suitable as a new class of implant material.

## 2.0 MATERIALS AND METHODS

A series of computed tomography (CT) image datasets of a craniofacial was used and analysed to develop a 3-D model of mandibular bone utilising an image-processing software, Mimics 20.0 (Materialise, Leuven, Belgium). Only one CT dataset of a real craniofacial considered in this study. The image datasets of CT scan were processed using appropriate scale of bone density to differentiate the distribution of the cortical and cancellous bone structures. The chosen region of interest is the posterior region of the left mandible covering the second premolar, first molar, and second molar tooth regions. The presence of the mandibular canal was ignored in this study. The constructed partial bone model was then compared with virtual mandibular bone model from 3-D human anatomy software which is Complete Anatomy from 3D4Medical, Elsevier, for accuracy. Several alterations have been made on the bone model including flattening the superior portion to avoid the development of highly distorted elements in that area. The completed bone model is 30-mm long, 20-mm high, 8- to 10-mm wide, and 2-mm thick (cortical layer). These dimensions are also consistent with those presented in several earlier computational works that considered similar bone region of interest [23, 24].

Considering the existence of the porous structure or also known as cancellous bone, it was designed as a solid continuum body with spongy material properties given. The cancellous bone was enclosed by the dense cortical layer. To simulate the insertion of the implant into the bone, the first molar tooth was removed representing a single restoration, while the remaining two teeth were neglected. The prosthesis or crown was modelled based on the enamel of anatomical configuration of the first molar using Boolean operation. The framework was also developed by scaling down the prosthesis model approximately 30%.

The 3-D model of the implant body, abutment, and abutment screw was developed in accordance with the dimensions of dual-fit implant (DFI) (Alpha-Bio Tec, Petach Tikva) using a computer-aided design software, SolidWorks 2020 (SolidWorks Corp., Concord, Massachusetts, USA). The diameter and length of the implant body are 3.75 and 11.5 mm, respectively. The implant-abutment morphology had been modelled as internal hexagonal connection and for the implant thread shape, the V-shaped type was imposed. The implant body was built as a one single body that would be attached to the abutment, and a screw was used to secure the abutment in place. The abutment is 3.5 mm in height, whilst the screw is 2.2 and 8 mm in width and length, respectively. All implant part models were generated using appropriate SolidWorks in-built geometry tools such as extrude, revolve, sweep, and/or loft. Model verification was made by comparing all the completed 3-D model designs with the actual dimensions and tolerances provided in the catalogue of implant manufacturer to

substantiate the model accuracy. Figure 1(a) depicts the exploded view of implant parts and bone models.

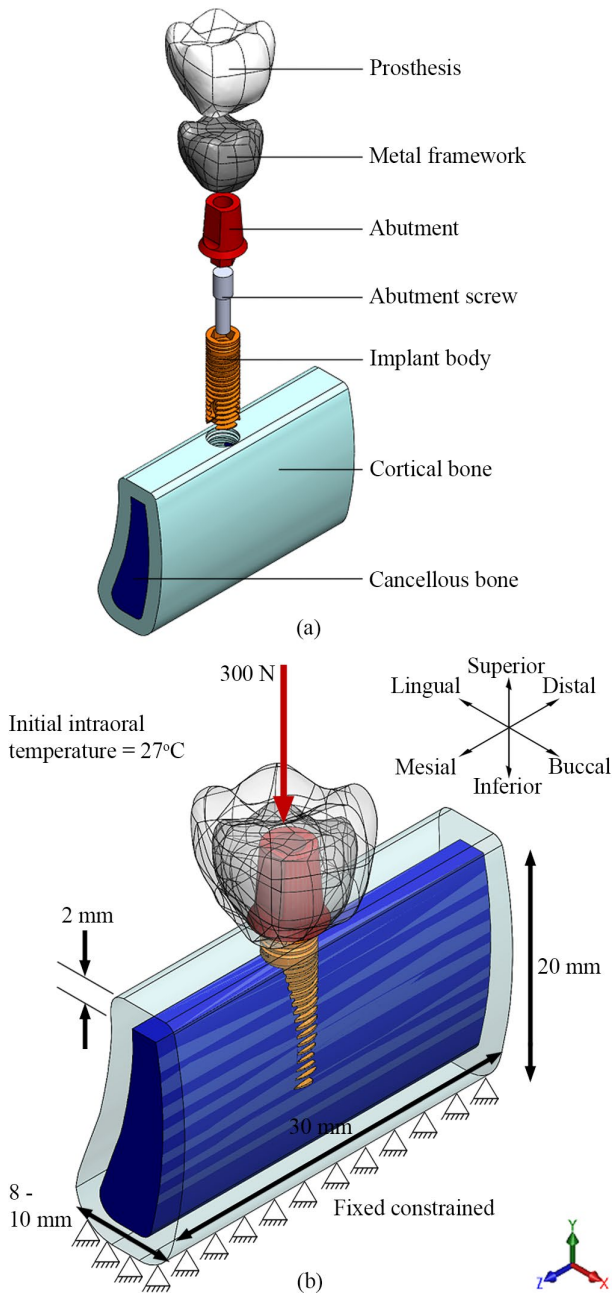


**Figure 1** (a) Exploded view of the implant system. (b) The boundary conditions showing rigid fixations at the bottom plane of the bone block and the occlusal force applied on the top surface of the prosthesis

All the constructed bone and implant component models were turned into solid geometry in SolidWorks software to establish the placement of the implant inside the bone. This was executed based on the recommended surgical procedures by Brånemark System®. Bone-level implant placement was selected in which the flat surface of implant platform and the top surface of the cortical bone was set parallel and positioned at the same level. This is also to ensure satisfactory prosthesis

orientation is achieved. “Combine” feature via “Subtract” tool was employed to succeed the development of 3.75-mm wide bone bed.

The contact between the implant body and the bones was assumed to be perfectly bonded designating a full osseointegration as frequently found in many previous *in-vitro* studies. It means that direct contact method was used to prevent any relative motion at the interface. The same approach was applied for the contact surfaces between the cortical and the cancellous bones. Whilst, all contact surfaces among implant and prosthetic parts were simulated via friction coefficient,  $\mu$  of 0.3 [25]. The contact algorithm adopted at the surfaces was Augmented Lagrange method which automatically controlled by the program. The contact detection occurred at Gauss integration point.

As mentioned earlier, the type of implant material must be taken into consideration in overloading as a trade-off between implant stability and load transfer is a key issue. In this study, 3-D FEA was performed on five different implant body material types – zirconia, Ti-6Al-4V, cpTi, TiZr, and PEEK – in terms of different elastic moduli,  $E$  and Poisson’s ratios,  $\nu$ . On the other hand, the abutment and abutment screw, prosthesis, and framework were made of Ti-6Al-4V, feldspathic porcelain, and cobalt-chromium (CoCr) alloy, respectively. They were kept constant throughout the analyses. The implant and prosthetic parts were modelled with isotropic properties, while the bones were assigned with anisotropic properties. The strength of the bone is primarily dependent on the orientation of collagen fibres in its structure. The elastic modulus of the cortical layer of the mandible is the highest along the mesio-distal direction ( $0^\circ$ , longitudinal), whilst the lowest along the corono-apical or bucco-lingual direction ( $90^\circ$ , transverse). Many recent analyses of anisotropic living tissue models have been of attention in order to acquire a more reliable result [26-28]. The material properties of all models used in the numerical analyses are defined in Table 1.

**Table 1** Young’s modulus and Poisson’s ratio for each finite element model

Material	Elastic Modulus, $E$ (GPa)	Poisson’s Ratio, $\nu$	Shear Modulus, $G$ (GPa)	References
Zirconia	200	0.3	-	[28]
Ti-6Al-4V	113.8	0.342	-	[23]
cpTi	110	0.35	-	[29]
TiZr	100	0.3	-	[28]
PEEK	18	0.39	-	[30]
Feldspathic porcelain	82.8	0.35	-	[12]
CoCr alloy	218	0.33	-	[10]
Cortical bone	$E_x = 17.9$ $E_y = 12.5$ $E_z = 26.6$	$\nu_{yz} = 0.31$ $\nu_{xy} = 0.26$ $\nu_{xz} = 0.28$	$G_{yz} = 5.3$ $G_{xy} = 4.5$ $G_{xz} = 7.1$	[27]
Cancellous bone	$E_x = 1.148$ $E_y = 0.021$ $E_z = 1.148$	$\nu_{yz} = 0.055$ $\nu_{xy} = 0.003$ $\nu_{xz} = 0.322$	$G_{yz} = 0.068$ $G_{xy} = 0.068$ $G_{xz} = 7.1$	[27]

The present study included two loading configurations – occlusal load and screw pretension. A dynamic occlusal force of 300 N [23] was subjected onto the top surface of the prosthesis along the longitudinal implant axis to represent chewing action.

For the pretension, a force of 20 N [23] was applied on the outer surface of the abutment screw. The initial environment or intraoral temperature was set to 27°C. In terms of structural boundary conditions, the bottom plane of the cortical bone model was fixedly constrained in the  $x$ ,  $y$ , and  $z$  directions to prevent any motions (translational and rotational displacements = 0) [23]. The loading and boundary conditions are illustrated in Figure 1(b).

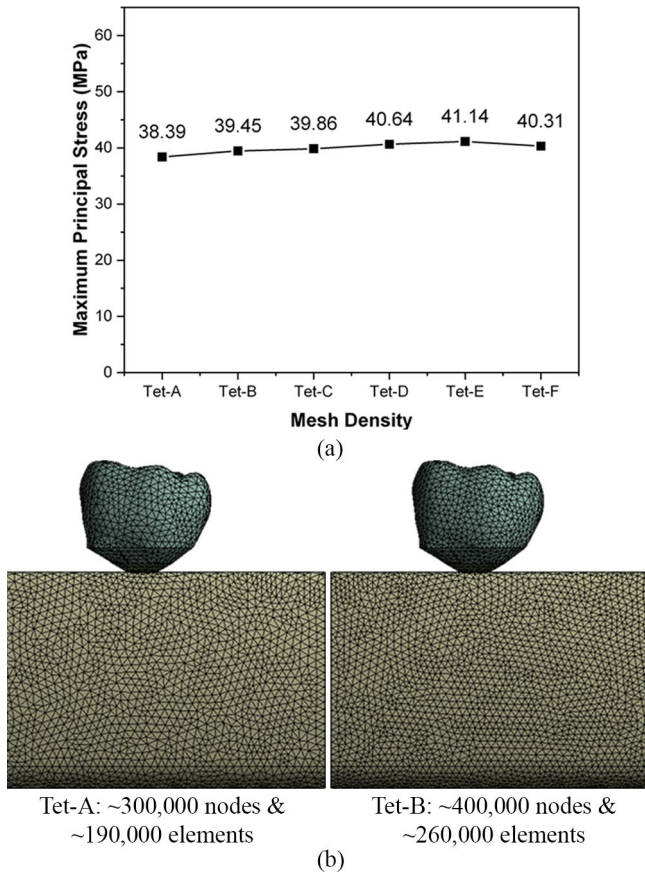


**Figure 2** (a) Maximum principal stress within the bone for different mesh densities (Tet-A – Tet-F). (b) Mesh configuration between Tet-A (before) and Tet-B (after one refinement)

The outcomes of FEA must be free from all purely numerical factors. Thus, it is important to conduct mesh convergence test. Prior to the convergence test, all models were turned into solid tetrahedral elements in ANSYS software (ANSYS Inc., Houston, TX, USA) with four nodes element type and three degrees of freedom. To perform the mesh convergence test, the model was set into several different number of elements with increasing mesh density. The total number of elements for each model set is Tet-A: 190,000 elements; Tet-B: 260,000 elements; Tet-C: 410,000 elements; Tet-D: 750,000 elements; Tet-E: 1,083,000 elements; and Tet-F: 1,690,000 elements. A. This work was done by utilising automatic solid meshing function in ANSYS software. The maximum principal stress results within the bone were analysed for all trials of the convergence test. The results exhibited that there was a little difference of the stress values recorded between the coarsest and the rest of the more refined models. The tetrahedral model appeared to converge with the highest change of 2.7% after one refinement which was about 260,000 elements and 400,000 nodes. Figure

2 shows a graph of maximum principal stress recorded within the bone and mesh configuration before (Tet-A) and after one refinement (Tet-B).

The proposed finite element model was also compared against previous related studies that assessing similar implant site and restoration type for verification purpose. The pre-processing settings applied in those studies were replicated except the model geometry. The comparison was made in terms of applicable response data type per selected study which is equivalent von Mises stress (MPa) within the bone. It was shown that the greatest stress level generated between our model with previous studies was less different and consistent (Table 2).

**Table 2** Comparison of maximum results between the literature and proposed models

Studies	Response	Literature Results	Model Results
Yalçın et al., (2019) [23]	Equivalent von Mises stress	Bone: 20.93 MPa	Bone: 29.93 MPa
Schwitalla et al., (2015) [24]	Equivalent von Mises stress	Bone: 17.00 MPa	Bone: 19.13 MPa

### 3.0 RESULTS

The results of analysis were presented in the form of maximum principal stress (bones), equivalent von Mises stress (implant body), maximum principal strain (bones), and total deformation (implant body-abutment assembly). Also, the data were described in colour contour plot with red indicating high stress, strain or total deformation value and blue indicating low value. Table 3 summarises the results of the analysis for each case.

**Table 3** Magnitudes of the stresses, strain, and total deformation recorded in all cases

Implant Body Material	Maximum Principal Stress (MPa)	Equivalent von Mises Stress (MPa)	Maximum Principal Strain	Total Deformation ( $\mu\text{m}$ )
Zirconia	39.66	736.84	4,985.1 $\mu$	104.14
Ti-6Al-4V	47.88	612.89	4,099.7 $\mu$	113.55
cpTi	48.27	602.79	4,035.2 $\mu$	114.03
TiZr	50.36	595.43	3,859.8 $\mu$	115.55
PEEK	141.81	265.42	13,612 $\mu$	174.89

As far as bone stress was concerned, the results depicted that the bone stress increased as the implant body stiffness was reduced, with PEEK recorded the highest stress value (141.81 MPa) as compared to zirconia (39.66 MPa), Ti-6Al-4V (47.88 MPa), cpTi (48.27 MPa), and TiZr (50.36 MPa). The maximum stress level generated in PEEK was found to be about 3.6-, 3.0-, 2.9-, and 2.8-fold greater than that in zirconia, Ti-6Al-4V, cpTi, TiZr, respectively. The area that was affected most by the excessive stresses was the cervical region on the distal side of the bone regardless of material type as illustrated in Figure

3. The critical region for PEEK implant was slightly close to the bone edge compared to others.

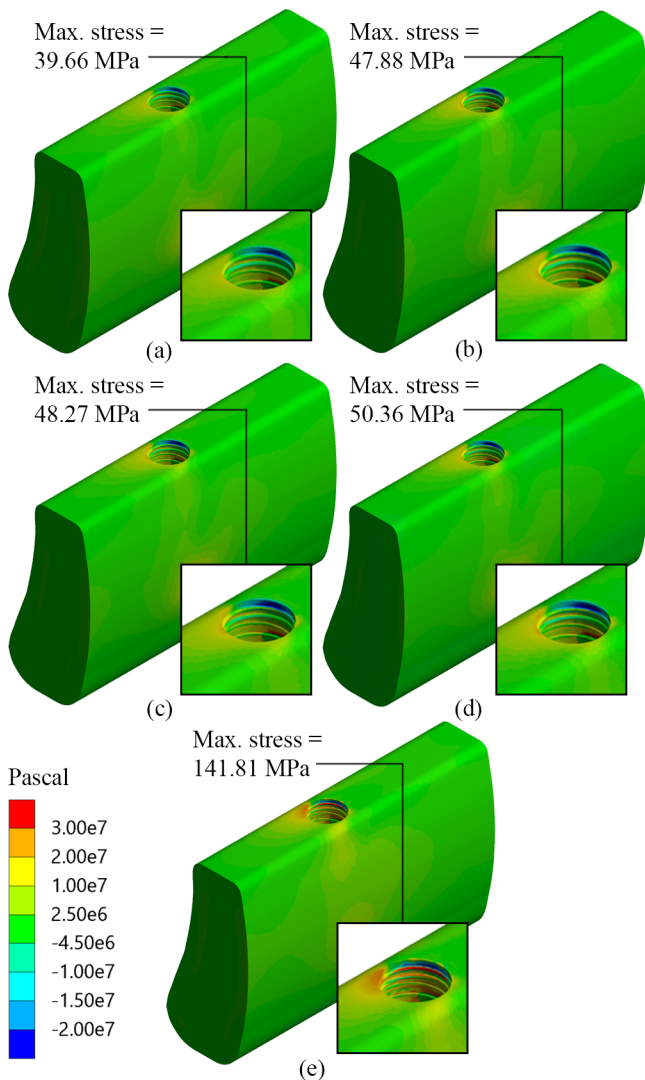


**Figure 3** Contour plots of maximum principal stress of the bones for different implant materials, (a) zirconia, (b) Ti-6Al-4V, (c) cpTi, (d) TiZr, and (e) PEEK

When the results were analysed for the implant body, it was evident that a contradict finding found where the stress was increased accordingly with the increase in implant stiffness. The maximum value of equivalent von Mises stress was recorded in zirconia implant (736.84 MPa) relative to others (Ti-6Al-4V: 612.89 MPa; cpTi: 602.79 MPa; TiZr: 595.43 MPa; PEEK: 265.42 MPa). The stress contour of the implant body exhibited a corresponding plot towards the bones. It demonstrated that the stresses were strongly concentrated at the inner distal edge of the implant platform before being progressively distributed in the corono-apical direction on the mesial side (Figure 4). As the stiffness was increased, the highly stressed region seemed to become wider towards the middle portion. More favourable stress dissipations were observed on the buccal, lingual and mesial sides, and apical portion regardless of the implant material. Among all materials, PEEK seemed to acquire the most adequate stress distribution in the implant body.

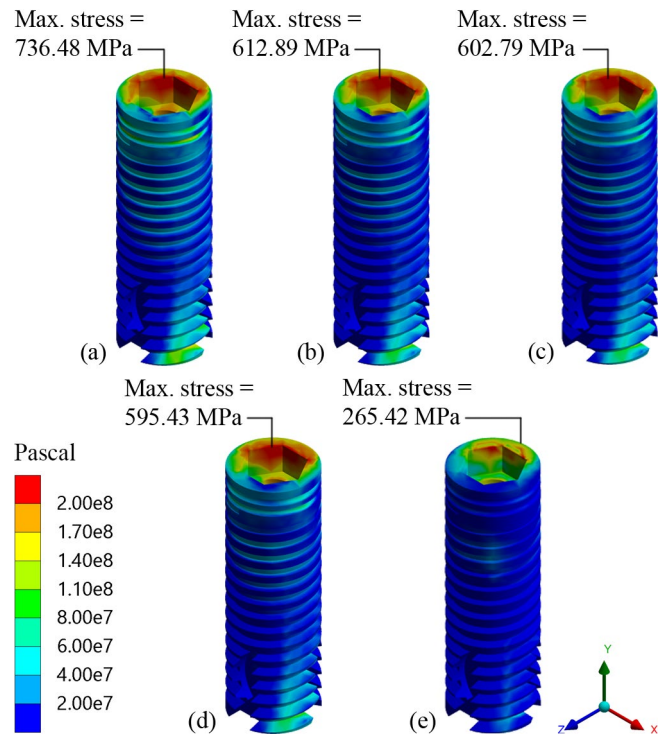


**Figure 4** Contour plots of equivalent von Mises stress of the implant body for different materials, (a) zirconia, (b) Ti-6Al-4V, (c) cpTi, (d) TiZr, and (e) PEEK

The results of maximum principal strain showed that there was a decrease in the bone strain in general when the stiffness of implant was reduced. However, the strain has considerably been increased for the implant with large difference of elastic modulus compared to others (PEEK). The PEEK implant (13,612  $\mu$ ) led to the greatest magnitude of bone strain compared with zirconia (4,985.1  $\mu$ ), Ti-6Al-4V (4,099.7  $\mu$ ), cpTi (4,035.2  $\mu$ ), and TiZr (3,859.8  $\mu$ ) implants, which increased by 63.4, 69.9, 70.4, and 71.6%, respectively. The strain values recorded in the cancellous bone were slightly higher than those recorded in the cortical bone regardless of implant materials except for PEEK implant. Strains of the bone were highly concentrated at the apical region of the implant on the lingual side as illustrated in Figure 5 for zirconia, Ti-6Al-4V, cpTi, and TiZr. Whilst, for PEEK implant, high strain intensity region was developed adjacent to the marginal bone area on the distal side. The strains were found to be more widespread for the cases with less stiff implants in almost all directions.

Depending on the material of the implant body, the value of implant-abutment assembly displacement increased proportionally as the low-stiffness implant was used. It was demonstrated that both abutment (zirconia: 104.14  $\mu$ m; Ti-6Al-4V: 113.55  $\mu$ m; cpTi: 114.03  $\mu$ m; TiZr: 115.55  $\mu$ m; PEEK: 174.89  $\mu$ m) and implant body (zirconia: 13.83  $\mu$ m; Ti-6Al-4V: 16.18  $\mu$ m; cpTi: 16.33  $\mu$ m; TiZr: 16.87  $\mu$ m; PEEK: 28.34  $\mu$ m) tend to highly displace as implant stiffness decreased. In comparison, the abutment displaced more than the implant body for all implant material types approximately from 83.8 (PEEK) up to 86.7% (zirconia) difference. This finding was expected due to the fact that the abutment has directly been loaded with the occlusal force (from the prosthesis) and pretension (on the abutment screw). Figure 6 exhibits a high deformation region occurred on

the distal side of the abutment and implant body. A smaller deformation concentration region developed at the medial and apical aspects, indicating a low tendency of the implant body to displace at those parts in all groups.

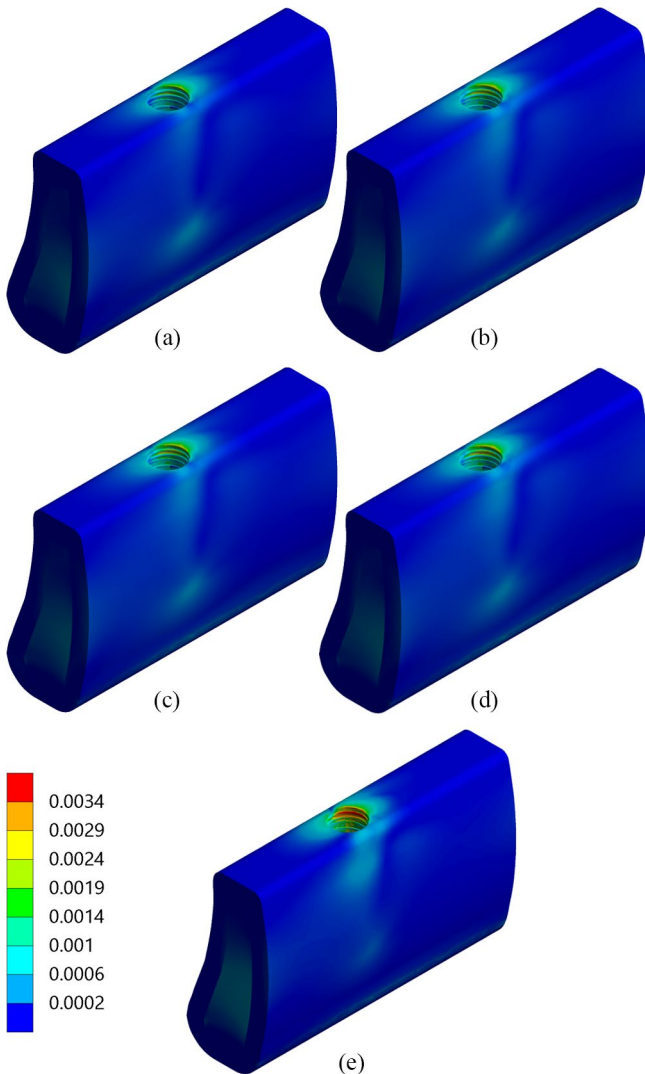


**Figure 5** Contour plots of maximum principal strain of the bones for different implant materials, (a) zirconia, (b) Ti-6Al-4V, (c) cpTi, (d) TiZr, and (e) PEEK

#### 4.0 DISCUSSION

The present study examined the influence of different implant body materials on a commercialised dental implant using 3-D FEA. The main goal was to analyse whether varying implant stiffness could affect bone adaptation limits and subsequently interfere the osseointegration. The clinical survival of a dental implant is substantially depending on primary stability and long-term osseointegration which yield lasting placement of the implant in the bone. The performance of dental implant is associated with many factors such as implant geometry, loading, fixation method, including material. Zirconia, Ti-6Al-4V, and cpTi are the most common materials used to make dental implants [8]. New emerging materials such as TiZr and PEEK have also been explored for possible implant applications [10,

28]. The effect of conventional and new materials on the load transfer within the system is important especially when the stress shielding effect is concerned. The mechanics of stress transfer at the bone-implant interface determines bone adaptation towards loading.

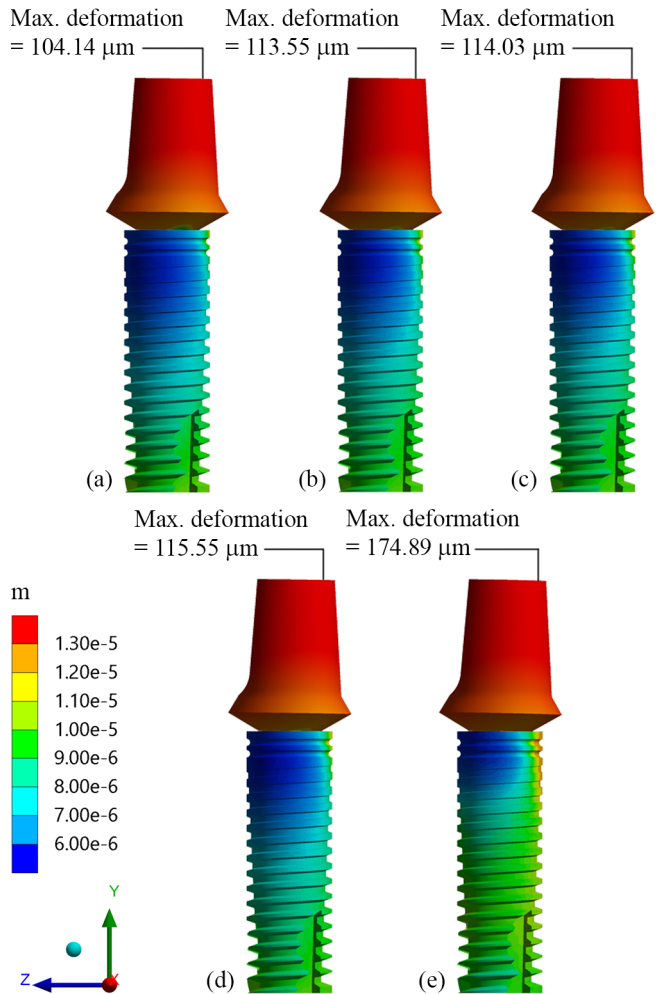


**Figure 6** Contour plots of total deformation of the implant-abutment assembly for different implant materials, (a) zirconia, (b) Ti-6Al-4V, (c) cpTi, (d) TiZr, and (e) PEEK

As far as stress within the bones was concerned, a greater stress magnitude was generally recorded for the less stiff implants compared to the stiffer ones. The reverse was seen for the implant body wherein the stress was significantly increased. These findings are probably due to the difference of stiffness between the implant body and the bone. From mechanical point of view, the implant material should have properties that almost similar to the contiguous bones to inhibit minimal bone adaptation stress. Generally, the significant difference in the value of Young's modulus between the metallic implant material (high) and the bone tissues (low) has caused the host bone to transfer the parafunctional and physiological loadings to the implant wherein this occurrence is known as stress shielding. The load and carrying capacity from the stiffer implant are shared with the bone. Subsequently, the loaded crestal bone will occupy less stresses and the remodelling process occurred. In this process, the degradation of bone is more dominant than the regeneration that leading to

the decrease in bone mass and quality. As a result, peri-prosthetic fracture may eventually occur. To associate the bone remodelling process with the measures quantified, Wolff's law is therefore concerned by evaluating the computed stresses [31]. The bone regions adjacent to the implant seem to sustain minimal stresses in comparison to the similar locations at the implant irrespective of material types as evidenced in this study. Flexible implants resulted in a higher stress within the bone than the stiff ones with PEEK implant demonstrated the most superior bone stress. The finding is consistent with a previous computational analysis by Bataineh & Al Janaideh (2019) [30]. They reported that carbon-fibre-reinforced PEEK implant yielded greater cortical bone stress than Ti-6Al-4V implant. Similar conclusion was found in another numerical study by Schwitalla et al. (2015) where PEEK implants increased the stress intensity in the peri-implant bone [24]. Although the bone stress level was increased, all the maximum magnitudes in all materials for this study are lower than the strength of the cortical bone, 170 MPa, including that of PEEK implant (141.81 MPa). For the implant body, the stress values recorded are considerably lower than the yield strength (YS) of some implant materials which are zirconia (~3-times lower; YS: 2000 MPa) and Ti-6Al-4V (~1.5-times lower; YS: 880 MPa). However, a contradicted finding was observed for cpTi (~1.3-times higher; YS: 480 MPa), TiZr (~2.6-times higher; YS: 230 MPa), and PEEK (~1.02-times higher; YS: 260 MPa) where the maximum implant stress magnitudes are greater than the yield strength of each corresponding material. The TiZr implant appears to be highly prone to failure compared to others. Of all materials, PEEK is observed to be the most favourable material in terms of bone and implant stress values and distributions. This could be explained by a comparable value of elastic modulus between PEEK and the bones which leaving insignificant stress shielding effect.

Apart from the mechanical stresses, strain intensity generated in the bones also plays an important role for the bone adaptation towards loading. Our results showed that the value of bone strain was generally decreased as the implant stiffness decreased. However, unexpected finding was noted when the bone strain has drastically been increased (13,612  $\mu$ ) for PEEK implant which having the lowest stiffness relative to others. Frost's mechanostat theory is applied to identify the association of the reported strains with bone reactions [32, 33]. The bone strains recorded by Ti-6Al-4V, cpTi, and TiZr implants exceeded 2,500  $\mu$  which signifying physiologic overload. In contrast, zirconia and PEEK implants predicting pathologic overload because the strain magnitudes were higher than 4,500  $\mu$ . This finding was in agreement with a past investigation that showed the undesirable strain values of the bones, expecting pathological bone failure [30]. The study reported that the level of bone strains for all contact surface types easily exceed 3,500  $\mu$  which do not correspond well with clinical observations. Different strain threshold classifications could be counted for different justifications of the alveolar bone strains.

Dental implant stability is termed as the ability of an implant system to be free from clinical mobility. Also, it is defined as the ability of an implant to withstand load in the axial and lateral directions, including rotational force. Both total deformations of the implant body and abutment observed in this study were increased with the decrease in the implant elastic modulus. The displacement of the implant body (13.83 – 28.34  $\mu$ m) regardless of material types appeared to lie within the range of

50 – 150  $\mu$ m [34] for an acceptable implant motion. The movement beyond this range could harm the bone-implant interface due to the formation of fibrous tissues. Flexible implants with the lower Young's modulus are expected to produce greater deformation than their stiffer counterpart. This has also generated a larger contact area between the implant and the bone which thus minimising stress dissipation in the implant body as being explained earlier.

Despite the robust findings, several aspects can further be improved such as applying tilting force during implant loading, using different types of implant body dimensions, and reversing implant extraction from the bony socket. This study had some limitations: (1) the simulated occlusal loading was only exerted at one specific point or node; (2) the gingiva soft tissue model was neglected; and (3) only the mandibular first molar tooth restoration was evaluated, meaning that the results can only be attributed to this group of teeth.

## 5.0 CONCLUSION

The results of simulated loadings and non-linear analysis support the following conclusions. The implant with a lower stiffness demonstrated an increased and a decreased stress level within the bones and implant body, respectively, compared to the implant with a higher stiffness. Besides, the less stiff implant also promoted lower strain and greater deformation values of the bones and implant-abutment assembly, respectively, than the stiffer implant. Of all materials evaluated, less stiff implants specifically PEEK implant is found to be the most favourable. However, relevant modifications on PEEK may be imposed to further enhance inherent bioactivity and osseointegration.

## Acknowledgement

The authors would like to acknowledge the support from Fundamental Research Grant Scheme (FRGS) under a grant number of FRGS/1/2020/TK0/UNIMAP/03/2 from the Ministry of Higher Education Malaysia. The authors reported no conflicts of interest related to this study.

## References

- [1] Pal, T. 2015. Fundamentals and History of Implant Dentistry. *Journal of International Clinical Dental Research Organization*. 7(3): 6-12. DOI: <https://doi.org/10.4103/2231-0754.172933>
- [2] Agustin-Panadero, R., Leon-Martinez, R., Labaig-Rueda, C., Faus-Lopez, J., and Sola-Ruiz, M. F. 2019. Influence of Implant-Prosthetic Connection on Peri-Implant Bone Loss: A Prospective Clinical Trial with 2-Year Follow-Up. *The International Journal of Oral & Maxillofacial Implants*. 34(4): 963-968. DOI: <https://doi.org/10.11607/jomi.7168>
- [3] Chrcanovic, B. R., Kisch, J., Albrektsson, T., and Wennerberg, A. 2018. Factors Influencing the Fracture of Dental Implants. *Clinical Implant Dentistry and Related Research*. 20(1): 58-67. DOI: <https://doi.org/10.1111/cid.12572>
- [4] Stoichkov, B. and Kirov, D. 2018. Analysis of the Causes of Dental Implant Fracture: A Retrospective Clinical Study. *Quintessence*

- International*. 49(4): 279-286. DOI: <https://doi.org/10.3290/j.qi.a39846>
- [5] Naveau, A., Shinmyouzu, K., Moore, C., Avivi-Arber, Jokerst, J., and Koka, S. 2019. Etiology and Measurement of Peri-Implant Crestal Bone Loss (CBL). *Journal of Clinical Medicine*. 8(2): 166. DOI: <https://doi.org/10.3390/jcm8020166>
- [6] Gupta, S., Gupta, H., and Tandan, A. 2015. Technical Complications of Implant-Causes and Management: A Comprehensive Review. *National Journal of Maxillofacial Surgery*. 6(1): 3-8. DOI: <https://doi.org/10.4103/0975-5950.168233>
- [7] Kunjappu, J., Mathew, V., Abdul Kader, M., Kuruniyan, M., Mohamed Ali, A., and Shamsuddin, S. 2019. Fracture of Dental Implants: An Overview. *International Journal of Preventive and Clinical Dental Research*. 6(1): 21-23. DOI: [https://doi.org/10.4103/inpc.inpc\\_27\\_19](https://doi.org/10.4103/inpc.inpc_27_19)
- [8] Farawati, F. A., and Nakaparksin, P. 2019. What is the Optimal Material for Implant Prosthesis? *Dental Clinics of North America*. 63(3): 515-530. DOI: <https://doi.org/10.1016/j.cden.2019.02.002>
- [9] Najeeb, S., Mali, M., Yaqin, S. A. U., Zafar, M. S., Khurshid, Z., Alwadaani, A., and Matinlinna, J. P. 2019. Chapter 21: Dental Implants Materials and Surface Treatments. *Advanced Dental Biomaterials*. 581-598.
- [10] Elias, D. M., Valerio, C. S., de Oliveira, D. D., Manzi, F. R., Zenóbio, E. G., and Seraidarian, P. I. 2020. Evaluation of Different Heights of Prosthetic Crowns Supported by an Ultra-Short Implant using Three-Dimensional Finite Element Analysis. *The International Journal of Prosthodontics*. 33(1): 81-90. DOI: <https://doi.org/10.11607/ijp.6247>
- [11] Siewert, B., Plaza-Castro, M., Sereno, N., and Jarman-Smith, M. 2019. Chapter 20 – Applications of PEEK in the Dental Field. *Peek Biomaterials Handbook*. 333-342.
- [12] Tekin, S., Değer, Y., and Demirci, F. 2019. Evaluation of the Use of PEEK Material in Implant-Supported Fixed Restorations by Finite Element Analysis. *Nigerian Journal of Clinical Practice*. 22(9): 1252-1258. DOI: [https://doi.org/10.4103/njcp.njcp\\_144\\_19](https://doi.org/10.4103/njcp.njcp_144_19)
- [13] Omar, A., Ishak, M. I., Harun, M. N., Sulaiman, E., and Kasim, N. H. A. 2012. Effects of Different Angulation Placement of Mini-Implant in Orthodontic. *Applied Mechanics and Materials*. 121-126: 1214-1219. DOI: <https://doi.org/10.4028/www.scientific.net/AMM.121-126.1214>
- [14] Ishak, M. I., Shafi, A. A., Rosli, M. U., Khor, C. Y., Zakaria, M. S., Rahim, W. M. F. W. A., and Jamalludin, M. R. 2017. Biomechanical Evaluation of Different Abutment-Implant Connections – A Nonlinear Finite Element Analysis. *AIP Conference Proceedings*. 1885(1): 020064. DOI: <https://doi.org/10.1063/1.5002258>
- [15] Ibrahim, M. I. F., Rosli, M. U., Ishak, M. I., Zakaria, M. S., Jamalludin, M. R., Khor, C. Y., Rahim, W. M. F. W. A., Nawi, M. A. M., and Shahrin, S. 2018. Simulation Based Optimization of Injection Molding Parameter for Meso-Scale Product of Dental Component Fabrication using Response Surface Methodology (RSM). *AIP Conference Proceedings*. 2030(1): 020078. DOI: <https://doi.org/10.1063/1.5066719>
- [16] Nawi, M. A. M., Razman Amin, M., Kasim, M. S., Izamshah, R., Ishak, M. I., Khor, C. Y., Rosli, M. U., Jamalludin, M. R., and Mohamad Syafiq, A. K. 2019. The Influence of Spiral Blade Distributor on Pressure Drop in a Swirling Fluidized Bed. *IOP Conference Series: Materials Science and Engineering*. 551(1): 012106. DOI: <https://doi.org/10.1088/1757-899x/551/1/012106>
- [17] Khor, C. Y., Ishak, M. I., Rosli, M. U., Jamalludin, M. R., Zakaria, M. S., Yamin, A. F. M., Abdul Aziz, M. S., and Abdullah, M. Z. 2017. Influence of Material Properties on the Fluid-Structure Interaction Aspects During Molded Underfill Process. *MATEC Web of Conferences*. 97: 01059. DOI: <https://doi.org/10.1051/mateconf/20179701059>
- [18] Abo Sabah, S., Kueh, A., and Bunnori, N. 2019. Failure Mode Maps of Bio-Inspired Sandwich Beams under Repeated Low-Velocity Impact. *Composites Science and Technology*. 182: 107785. DOI: <https://doi.org/10.1016/j.compscitech.2019.107785>
- [19] Hanif, M. U., Ibrahim, Z., Ghaedi, K., Javanmardi, A., and Rehman, S. K. 2018. Finite Element Simulation of Damage in RC Beams. *Journal of Civil Engineering, Science and Technology*. 9(1): 50-57. DOI: <https://doi.org/10.33736/jcest.883.2018>
- [20] Ghaedi, K., Ibrahim, Z., Javanmardi, A., Jameel, M., Hanif, U., Rehman, S. K., and Gordan, M. 2018. Finite Element Analysis of a Strengthened Beam Deliberating Elastically Isotropic and Orthotropic CFRP Material. *Journal of Civil Engineering, Science and Technology*. 9(2): Paper 5. DOI: <https://doi.org/10.33736/jcest.991.2018>
- [21] Al-Fasih, M. Y., Kueh, A. B. H., Abo Sabah, S. H., and Yahya, M. Y. 2018. Tow Waviness and Anisotropy Effects on Mode II Fracture of Triaxially Woven Composite. *Steel and Composite Structures*. 26(2): 241-253. DOI: <https://doi.org/10.12989/scs.2018.26.2.241>
- [22] Al-Fasih, M. Y., Kueh, A. B. H., Abo Sabah, S. H., and Yahya, M. Y. 2017. Influence of Tows Waviness and Anisotropy on Effective Mode I Fracture Toughness of Triaxially Woven Fabric Composites. *Engineering Fracture Mechanics*. 182: 521-536. DOI: <https://doi.org/10.1016/j.engfracmech.2017.03.051>
- [23] Yalçın, M., Kaya, B., Laçın, N., and Arı, E. 2019. Three-Dimensional Finite Element Analysis of the Effect of Endosteal Implants with Different Macro Designs on Stress Distribution in Different Bone Qualities. *The International Journal of Oral & Maxillofacial Implants*. 34(3): e43–e50. DOI: <https://doi.org/10.11607/jomi.7058>
- [24] Schwitala, A. D., Abou-Emara, M., Spintig, T., Lackmann, J., and Müller, W. D. 2015. Finite Element Analysis of the Biomechanical Effects of Peek Dental Implants on the Peri-Implant Bone. *Journal of Biomechanics*. 48(1): 1-7. DOI: <https://doi.org/10.1016/j.jbiomech.2014.11.017>
- [25] Tribst, J. P. M., Dal Piva, A. M. d. O., Borges, A. L. S., and Bottino, M. A. 2020. Influence of Socket-Shield Technique on the Biomechanical Response of Dental Implant: Three-Dimensional Finite Element Analysis. *Computer Methods in Biomechanics and Biomedical Engineering*. 23(6): 224-231. DOI: <https://doi.org/10.1080/10255842.2019.1710833>
- [26] Hudieb, M. I., Wakabayashi, N., Abu-Hammad, O. A., and Kasugai, S. 2019. Biomechanical Effect of an Exposed Dental Implant's First Thread: A Three-Dimensional Finite Element Analysis Study. *Medical Science Monitor*. 25: 3933-3940. DOI: <https://doi.org/10.12659/msm.913186>
- [27] Robau-Porrúa, A., Pérez-Rodríguez, Y., Soris-Rodríguez, L. M., Pérez-Acosta, O., and González, J. E. 2020. The Effect of Diameter, Length and Elastic Modulus of a Dental Implant on Stress and Strain Levels in Peri-Implant Bone: A 3D Finite Element Analysis. *Bio-Medical Materials and Engineering*. 30: 541-558. DOI: <https://doi.org/10.3233/BME-191073>
- [28] Tretto, P. H. W., dos Santos, M. B. F., Spazzin, A. O., Pereira, G. K. R., and Bacchi, A. 2020. Assessment of Stress/Strain in Dental Implants and Abutments of Alternative Materials Compared to Conventional Titanium Alloy – 3D Non-Linear Finite Element Analysis. *Computer Methods in Biomechanics and Biomedical Engineering*. 23(8): 372-383. DOI: <https://doi.org/10.1080/10255842.2020.1731481>
- [29] Brune, A., Stiesch, M., Eisenburger, M., and Greuling, A., 2019. The Effect of Different Occlusal Contact Situations on Peri-Implant Bone Stress – A Contact Finite Element Analysis of Indirect Axial Loading. *Materials Science and Engineering: C*. 99: 367-373. DOI: <https://doi.org/10.1016/j.msec.2019.01.104>
- [30] Bataineh, K., and Al Janaideh, M. 2019. Effect of Different Biocompatible Implant Materials on the Mechanical Stability of Dental Implants under Excessive Oblique Load. *Clinical Implant*

- Dentistry and Related Research*. 21(6): 1206-1217. DOI: <https://doi.org/10.1111/cid.12858>
- [31] Sego, T. J. 2016. Finite Element Analysis of and Multiscale Skeletal Tissue Mechanics Concerning a Single Dental Implant Site. *Thesis (Master), Purdue University, Ann Arbor, Michigan, United States of America*.
- [32] Dantas, T. A., Carneiro Neto, J. P., Alves, J. L., Vaz, P. C. S., and Silva, F. S. 2020. In Silico Evaluation of the Stress Fields on the Cortical Bone Surrounding Dental Implants: Comparing Root-Analogue and Screwed Implants. *Journal of the Mechanical Behavior of Biomedical Materials*. 104: 103667. DOI: <https://doi.org/10.1016/j.jmbbm.2020.103667>
- [33] Matsuzaki, T., Ayukawa, Y., Matsushita, Y., Sakai, N., Matsuzaki, M., Masuzaki, T., Haraguchi, T., Ogino, Y., and Koyano, K. 2019. Effect of Post-Osseointegration Loading Magnitude on the Dynamics of Peri-Implant Bone: A Finite Element Analysis and In Vivo Study. *Journal of Prosthodontic Research*. 63(4): 453-459. DOI: <https://doi.org/10.1016/j.jpor.2018.10.009>
- [34] Dorogoy, A., Rittel, D., Shemtov-Yona, K., and Korabi, R. 2017. Modeling Dental Implant Insertion. *Journal of the Mechanical Behavior of Biomedical Materials*. 68: 42-50. DOI: <https://doi.org/10.1016/j.jmbbm.2017.01.021>